Mineralogical Magazine, February 2017, Vol. 81(1), pp. 35–46

Bohseite, ideally $Ca_4Be_4Si_9O_{24}(OH)_4$, from the Piława Górna quarry, the Góry Sowie Block, SW Poland

E. Szełęg[1], B. Zuzens[2], F. C. Hawthorne[2,*], A. Pieczka[3], A. Szuszkiewicz[4], K. Turniak[4], K. Nejbert[5], S. S. Ilnicki[5], H. Friis[6], E. Makovicky[7], M. T. Weller[8] and M.-H. Lemée-Cailleau[9]

[1] Department of Geochemistry, Mineralogy and Petrography, University of Silesia, Będzińska 60, 41-200 Sosnowiec, Poland
[2] Department of Geological Sciences, University of Manitoba, Winnipeg, Manitoba R3T 2N2, Canada
[3] Department of Mineralogy, Petrography and Geochemistry, AGH University of Science and Technology, Mickiewicza 30, 30-059 Kraków, Poland
[4] University of Wrocław, Institute of Geological Sciences, Cybulskiego 30, 50-205 Wrocław, Poland
[5] Institute of Geochemistry, Mineralogy and Petrology, University of Warsaw, Żwirki and Wigury 93, 02-089 Warszawa, Poland
[6] Natural History Museum, University of Oslo, Postboks 1172, Blindern, 0318 Oslo, Norway
[7] Department of Geosciences and Natural Resources, University of Copenhagen, Rolighedsvej 23, 1958 Frederiksberg, Denmark
[8] Department of Chemistry, University of Bath, Bath BA2 7AY, UK
[9] Institut Laue-Langevin, B.P.156, 6 rue Jules Horowitz, 38042 Grenoble Cedex 9, France

[*Received 6 April 2015; Accepted 1 December 2015; Associate Editor: Ed Grew*]

ABSTRACT

Bohseite is an orthorhombic calcium beryllium aluminosilicate with variable Al content and an end-member formula $Ca_4Be_4Si_9O_{24}(OH)_4$, that was discovered in the Piława Górna quarry in the eastern part of the Góry Sowie Block, ~50 km southwest of Wrocław, SW Poland. It occurs in a zoned anatectic pegmatite dyke in close association with microcline, Cs-rich beryl, phenakite, helvite, 'lepidolite', probably bertrandite and unidentified Be-containing mica as alteration products after a primary Be mineral, probably beryl. Bohseite forms fan-like or parallel aggregates (up to 0.7 cm) of white, platy crystals (up to 2 mm long) with characteristic striations. It is white with a white streak, is translucent and has a vitreous lustre; it does not fluoresce under ultraviolet light. The cleavage is perfect on {001} and fair on {010}, and neither parting nor twinning was observed. Bohseite is brittle with a splintery fracture and Mohs hardness is 5–6. The calculated density is 2.719 g cm^{-3}. The indices of refraction are $\alpha = 1.579$, $\beta = 1.580$, $\gamma = 1.597$, all ±0.002; 2Vobs = 24(3)°, 2Vcalc = 27°; the optic orientation is as follows: X ^ **a** = 16.1°, Y ^ **b** = 16.1°, Z // **c**. Bohseite shows orthorhombic diffraction symmetry, space group *Cmcm*, $a = 23.204(6)$, $b = 4.9442(9)$, $c = 19.418(6)$ Å, $V = 2227.7(4)$ Å^3, $Z = 4$. The crystal structure was refined to an R_1 value of 2.17% based on single-crystal data, and the chemical composition was determined by electron-microprobe analysis. Bohseite is isostructural with bavenite. Bohseite was originally approved with an end-member composition of $Ca_4Be_3AlSi_9O_{25}(OH)_3$, but subsequent discovery of compositions with Be > 3.0 apfu led to redefinition of its end-member composition, holotype sample and locality, as reported here. There is extensive solid solution in bavenite–bohseite according to the scheme $^{O(2)}OH^- + {}^{T(4)}Si^{4+} + {}^{T(3)}Be^{2+} \leftrightarrow {}^{O(2)}O^{2-} + {}^{T(4)}Al^{3+} + {}^{T(3)}Si^{4+}$, and a general formula for the bavenite–bohseite minerals may be written as $Ca_4Be_xSi_9Al_{4-x}O_{28-x}(OH)_x$, where x ranges from 2–4 apfu: $Ca_4Be_2Si_9Al_2O_{26}(OH)_2$ (bavenite) to $Ca_4Be_4Si_9O_{24}(OH)_4$ (bohseite).

*E-mail: frank_hawthorne@umanitoba.ca
https://doi.org/10.1180/minmag.2016.080.066

Keywords: bohseite, bavenite, crystal-structure refinement, infrared spectrum, electron-microprobe analysis, beryllium, end-member, solid-solution.

Introduction

Bavenite is a calcium beryllium aluminosilicate mineral occurring primarily in granitic pegmatites (Černý, 2002) and is a widespread product of hydrothermal alteration, particularly of beryl (Černý, 1968; Bondi *et al.*, 1983). Detailed chemical compositions were given by Switzer and Reichen (1960), Berry (1963), Beus (1966) and Cannillo *et al.* (1966), and both Cannillo *et al.* (1966) and Kharitonov *et al.* (1971) showed that the crystal structure is a framework of silicate and beryllate tetrahedra with the general formula $Ca_4[Be_{(2+x)}Al_{(2-x)}][Si_9O_{(26-x)}(OH)_{(2+x)}]$. Beus (1966) wrote the bavenite series as between the compositions $Ca_4Be_2Al_2Si_9O_{26}(OH)_2$ and $Ca_4Be_3AlSi_9O_{25}(OH)_3$. The composition $Ca_4Be_2Al_2Si_9O_{26}(OH)_2$ was accepted as the end-member formula of bavenite, and the name bohseite was given recently to the composition $Ca_4Be_3AlSi_9O_{25}(OH)_3$ (Friis *et al*., 2010). Lussier and Hawthorne (2011) presented data for compositions with Be ~3.1 apfu, slightly beyond the limit of Be = 3 apfu suggested for bohseite, and since then we have found compositions with Be ~3.5 (structural refinement) and ~3.8 apfu calculated by stoichiometry from electron microprobe analysis, considerably beyond the originally accepted limit of Be = 3 apfu for bohseite. These data indicate that the Be-rich end-member for these compositions is as proposed by Lussier and Hawthorne (2011): $Ca_4Be_4Si_9O_{24}(OH)_4$. Rather than having a new name, it seems more reasonable to redefine the end-member composition, the compositional range of bohseite, and the locality of the holotype material in accord with the data presented here. The original proposal was approved by the IMA-CNMMN as IMA 2010-026; this redefinition was approved by the IMA-CNMNC, nomenclature-voting proposal 14-H. Type material is deposited at the Mineralogical Museum, University of Wrocław, catalogue numbers: holotype: MMUWr IV7678.; cotype: MMUWr IV7679. The original material proposed as IMA 2010-026 is from the Ilímaussaq alkaline complex, South Greenland, and material is stored at the Natural History Museum in Copenhagen, Denmark (GM 1995.32) (Friis *et al.*, 2010). The material was investigated by Petersen *et al.* (1995) and Armstrong *et al.* (2010). The name is in honour of the Danish geologist Hennning Bohse (1942 – present) who has worked for more than 40 years on the mineralogy and geology of the Ilímaussaq alkaline complex.

Occurrence

Bohseite occurs in the most strongly fractionated part of a mixed NYF (Nb-Y-F) + LCT (Li-Cs-Ta) co-genetic pegmatite system exposed in the Piława Górna migmatite-amphibolite quarry worked by the Dolnośląskie Surowce Skalne S.A Company in the eastern part of the Góry Sowie Block, ~50 km southwest of Wrocław, SW Poland (50°42′11.77″N; 16°44′12.36″E) (NE part of the Bohemian massif). The tectonized amphibolites are cut discordantly by anatectic zoned pegmatite dykes, with individual dimensions reaching 30–40 m in vertical section, 80–100 m in longitudinal section and 6 m thick (Szełęg *et al.*, 2010; Pieczka *et al.*, 2012, 2013; Szuszkiewicz *et al.*, 2013). Pegmatites of the system typically display a zoned internal structure (border zone + wall zone + graphic intermediate zone + blocky-feldspar intermediate zone + quartz core ± quartz-albite zone ± spodumene-'lepidolite' core) with usually low to moderate degrees of geochemical fractionation and enhanced Nb–*REE*–Be–B contents. They consist mainly of microcline, plagioclase ('oligoclase'-'andesine' and albite), quartz, biotite and muscovite accompanied by schorl, garnet (almandine–spessartine series) and beryl. Rare-element minerals are

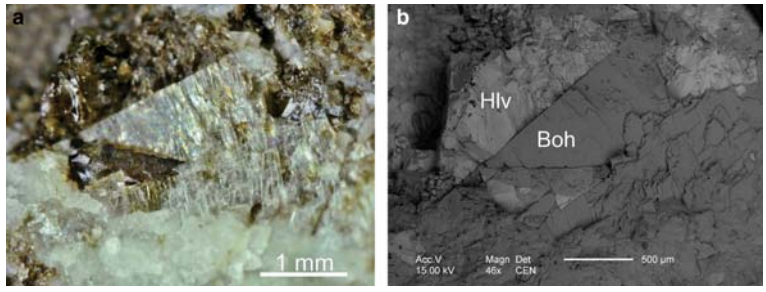

Fig. 1. (*a*) Aggregate of bohseite crystals; (*b*) Back-scatter electron image of bohseite (Boh) and adjacent helvite (Hlv).

TABLE 1. Two-dimensional diffraction pattern for bohseite.

I_{rel}	$d^*_{(pattern)}$ (Å)	$d^*_{(peak)}$ (Å)	h	k	l	I_{rel}	$d_{(pattern)}$ (Å)	$d_{(peak)}$ (Å)	h	k	l
9	7.446	7.446	2	0	2	11	2.097	2.097	3	1	8
11	4.980	4.980	4	0	2		–	2.097	7	1	6
4	4.855	4.855	0	0	4		–	2.094	10	0	4
	–	4.836	1	1	0	7	2.083	2.085	0	2	5
3	4.478	4.478	2	0	4		–	2.083	6	2	0
9	4.328	4.329	1	1	2	15	2.068	2.068	9	1	4
38	4.166	4.166	3	1	0	13	1.971	1.972	5	1	8
3	4.079	4.073	3	1	1		–	1.970	1	1	9
12	3.869	3.874	1	1	3		–	1.970	9	1	5
	–	3.867	6	0	0	11	1.940	1.942	0	0	10
11	3.829	3.828	3	1	2		–	1.937	2	2	6
51	3.723	3.723	4	0	4	9	1.914	1.915	2	0	10
2	3.594	3.593	6	0	2		–	1.914	6	2	4
44	3.383	3.384	5	1	0	9	1.867	1.867	9	1	6
100	3.334	3.334	5	1	1	5	1.847	1.847	8	2	2
28	3.236	3.236	0	0	6	8	1.819	1.823	2	2	7
25	3.196	3.195	5	1	2		–	1.821	7	1	8
18	3.117	3.117	2	0	6		–	1.819	5	1	9
37	3.027	3.028	1	1	5	16	1.753	1.754	8	2	4
	–	3.025	6	0	4		–	1.752	6	2	6
18	2.999	2.999	5	1	3	18	1.736	1.736	11	1	5
17	2.840	2.841	3	1	5		–	1.735	6	0	10
5	2.779	2.779	8	0	2	3	1.693	1.693	8	2	5
	–	2.776	5	1	4		–	1.692	10	2	0
2	2.754	2.753	7	1	0	3	1.677	1.677	10	0	8
5	2.726	2.726	7	1	1		–	1.673	13	1	1
5	2.649	2.649	7	1	2	13	1.659	1.660	12	0	6
31	2.553	2.556	3	1	6		–	1.660	4	2	8
	–	2.551	5	1	5		–	1.657	14	0	0
16	2.535	2.534	7	1	3	8	1.638	1.638	1	3	1
8	2.482	2.490	8	0	4		–	1.637	10	2	3
	–	2.482	6	0	6		–	1.634	14	0	2
4	2.452	2.452	0	2	1	7	1.629	1.627	8	2	6
14	2.405	2.406	1	1	7		–	1.626	0	2	9
	–	2.399	2	2	1		–	1.625	3	1	11
3	2.378	2.376	2	0	8		–	1.625	13	1	3
3	2.346	2.346	2	2	2	7	1.618	1.618	0	0	12
4	2.320	2.320	10	0	0	3	1.607	1.606	3	3	1
19	2.266	2.270	9	1	1		–	1.603	2	0	12
	–	2.265	2	2	3	5	1.587	1.590	3	3	2
14	2.246	2.246	7	1	5		–	1.590	11	1	7
6	2.226	2.225	9	1	2		–	1.587	7	1	10
8	2.203	2.203	0	2	4	9	1.566	1.569	9	1	9
3	2.165	2.169	1	1	8			1.569	14	0	4
	–	2.164	2	2	4			1.590	4	2	9
	–	2.160	8	0	6			1.565	5	1	11
7	2.145	2.146	4	2	3			1.565	3	3	3
	–	2.145	5	1	7						

*$d_{(peak)}$ gives the d-value for that specific h k l; $d_{(pattern)}$ gives the d-value for the aggregate envelope.

represented by columbite-group minerals, ixiolite, ferrowodginite, samarskite-, euxenite- and fergusonite-group minerals, pyrochlore-supergroup minerals, Nb- and Ta-enriched varieties of cassiterite, ilmenite and titanite, gadolinite-group minerals, hellandite-(Y), keiviite-(Y), allanite-(Y), allanite-(Ce), ferriallanite-(Ce), xenotime-(Y), monazite-(Ce) and many others (a complete list is given by Szuszkiewicz *et al.*, 2013), suggesting NYF affiliation for the parental melt. In the axial parts of the largest dykes, there are signs of more- and much-more strongly fractionated Li–Cs–Ta–Be–B mineralization of the LCT type, which only formed exceptionally as larger pods. Bohseite, of atypical composition in relation to that of Friis *et al.* (2010), comes from the largest such pod (exposed in the quarry by mining in 2010), probably a dozen metres in diameter, with a visible Li- and Cs-mineralized graphic intermediate zone, a blocky feldspar zone, a quartz-albite zone and a spodumene + 'lepidolite' core (Szełęg *et al.*, 2013). Typical components of the LCT part of the pegmatite are microcline, albite, quartz, 'lepidolite', spodumene, pollucite, cassiterite, spessartine, tantalite-(Mn), minerals of the microlite group, elbaite – liddicoatite – rossmanite, Cs-bearing beryl and pezzottaite, Cs-bearing dark mica and sokolovaite. In various veins and dykes, beryl is commonly altered to bavenite, forming rosettes some millimetres across (up to 1 cm). In the LCT part, bohseite is associated closely with microcline, Cs-rich beryl, phenakite, helvite, 'lepidolite', bertrandite and unidentified Be-containing mica-like minerals as alteration products after a primary Be mineral, probably beryl.

Many pegmatite veins and dykes in the Góry Sowie Block are of anatectic origin and formed during melting of the metasedimentary-metavolcanic protolith ~380–370 Ma (van Breemen *et al.*, 1988; Timmermann *et al.*, 2000). During their formation, some unusual geochemical processes occurred, producing: (1) a distinct reversal in Mn–Fe fractionation trends in the columbite-group minerals; (2) enrichment in Fe, Sn, Sc and mainly in Ti visible in the evolution of columbite-group minerals to Ti- or Sn-bearing ixiolite, crystallization of ferrowodginite, crystallization of samarskite-group minerals before euxenite-group minerals and fergusonite-(Y), and crystallization of bi-coloured tourmaline crystals with a blue core (with negligible Ti) and an olive-brown to brown mantle distinctly enriched in Ti (Fe/Ti ratios decrease from 120 to 10 from the core to the outermost zone); (3) Ca metasomatism involving replacement of spessartine by Ca-bearing spessartine, gradual enrichment of ishikawaite, samarskite-(Y) and polycrase-(Y) in Ca, with final alteration of Nb-Ta phases to Ca-bearing pyrochlore-supergroup minerals, alteration of beryl to members of the bavenite–bohseite series, crystallization of tiny epidote-group minerals in thin veinlets cutting the feldspars and crystallization of titanite (Pieczka *et al.*, 2013, 2014). Bohseite, found in the most evolved part of the pegmatites, in the mineral assemblage as described above, suggests late crystallization under the influence of Ca-enriched fluids in a residual pegmatite environment with extremely high Be activity relative to Al activity.

Physical properties

Bohseite forms fan-like or parallel aggregates of white, platy crystals (up to 2 mm long) with characteristic striations, and aggregates reach sizes up to 0.7 cm (Fig. 1). Bohseite is white with a white streak, is translucent and has a vitreous lustre; it does not fluoresce under ultraviolet light. The cleavage is perfect on {001} and fair on {010}, and no parting or twinning was observed. The Mohs hardness is 5–6 and bohseite is brittle with a splintery fracture. The density was not measured due to the paucity of material and its high degree of chemical zoning. The calculated density is 2.719 gcm^{-3}. Optical properties were measured with a Bloss spindle stage for the wavelength 590 nm. The indices of refraction are $\alpha = 1.579$, $\beta = 1.580$, $\gamma = 1.597$, all ± 0.002; $2V_{obs} = 24(3)°$; data processed using *Excalibr II* (Bartelmehs *et al.*, 1992), $2V_{calc} = 27°$; the dispersion is $r < v$, weak. The optic orientation (determined by transferring the optics crystal from the spindle stage to a

TABLE 2. Data-collection information for the crystal structure of bohseite.

a (Å)	23.204(6)
b (Å)	4.9442(9)
c (Å)	19.418(6)
V (Å^3)	2227.7
R_1	2.17
wR_2	5.85
Goof	1.014
Reflections collected	12,944
Reflections merged	1709
$\Sigma \lvert Fo \rvert > 4\sigma F$	1532
R_{int}	3.03
Crystal dimensions (μm)	25 × 10 × 55

TABLE 3. Representative chemical compositions (wt.%) of selected bohseite crystals from the Piława Górna quarry, Poland.

	1	2	3	4	5	6	7	8	9	10	11	12	13	14	15	16	17
wt.%																	
SiO_2	59.11	58.39	58.20	58.62	59.17	59.31	58.90	59.47	59.27	59.07	59.07	58.75	59.10	58.32	58.41	58.86	58.04
Al_2O_3	6.49	6.00	5.89	4.80	4.06	3.75	3.24	2.92	2.77	2.74	2.71	2.66	2.57	2.64	2.57	2.04	1.87
CaO	24.45	24.53	24.66	24.52	24.60	24.50	24.58	24.57	24.46	24.57	24.60	24.59	24.74	24.65	24.73	24.72	24.96
Na_2O	0.04	0.04	0.03	0.06	0.09	0.13	0.09	0.09	0.10	0.08	0.09	0.09	0.07	0.09	0.11	0.01	0.02
F_2	0.20	0.39	0.32	0.60	0.47	0.54	0.51	0.41	0.44	0.58	0.51	0.52	0.38	0.51	0.33	0.33	0.69
$BeO_{(calc.)}$	7.75	8.03	8.14	8.63	9.06	9.19	9.45	9.59	9.63	9.68	9.72	9.73	9.83	9.77	9.86	10.03	10.24
$H_2O_{(calc.)}$	2.71	2.68	2.73	2.81	3.04	3.08	3.15	3.28	3.28	3.21	3.25	3.24	3.34	3.24	3.35	3.42	3.26
$-O=F_2$	–0.08	–0.16	–0.13	–0.25	–0.20	–0.23	–0.21	–0.17	–0.19	–0.24	–0.21	–0.22	–0.16	–0.21	–0.14	–0.14	–0.29
Totals	100.65	99.90	99.81	99.79	100.29	100.27	99.71	100.15	99.77	99.69	99.73	99.36	99.87	98.98	99.22	99.28	98.78
28 anions with Be = 13–(Si + Al) and Ca + Na = Al + Be (Lussier & Hawthorne, 2011)																	
Ca^{2+}	3.99	4.03	4.06	4.02	4.00	3.98	4.01	3.98	3.98	4.00	4.00	4.02	4.02	4.04	4.05	4.03	4.10
Na^{+}	0.01	0.01	0.01	0.02	0.03	0.04	0.03	0.03	0.03	0.02	0.03	0.03	0.02	0.03	0.03	0.00	0.01
Ca+Na	**4.00**	**4.04**	**4.07**	**4.04**	**4.03**	**4.01**	**4.04**	**4.01**	**4.01**	**4.02**	**4.03**	**4.04**	**4.04**	**4.07**	**4.08**	**4.04**	**4.11**
Al^{3+}	1.16	1.09	1.07	0.87	0.73	0.67	0.58	0.52	0.50	0.49	0.48	0.48	0.46	0.48	0.46	0.37	0.34
Be^{2+}	2.84	2.96	3.00	3.17	3.30	3.34	3.45	3.49	3.51	3.53	3.54	3.56	3.58	3.59	3.62	3.67	3.77
Al+Be	**4.00**	**4.00**	**4.00**	**4.00**	**4.00**	**4.00**	**4.00**	**4.00**	**4.00**	**4.00**	**4.00**	**4.00**	**4.00**	**4.00**	**4.00**	**4.00**	**4.00**
Si^{4+}	9.00	8.96	8.93	8.96	8.97	8.99	8.96	8.99	8.99	8.98	8.97	8.96	8.96	8.93	8.92	8.96	8.89
Al^{3+}	0.00	0.04	0.07	0.04	0.03	0.01	0.04	0.01	0.01	0.02	0.03	0.04	0.04	0.07	0.08	0.04	0.11
Si+Al	**9.00**	**9.00**	**9.00**	**9.00**	**9.00**	**9.00**	**9.00**	**9.00**	**9.00**	**9.00**	**9.00**	**9.00**	**9.00**	**9.00**	**9.00**	**9.00**	**9.00**
F^{-}	0.10	0.19	0.15	0.29	0.23	0.26	0.25	0.20	0.21	0.28	0.24	0.25	0.18	0.25	0.16	0.16	0.34
OH^{-}	2.75	2.74	2.79	2.86	3.08	3.11	3.20	3.31	3.32	3.25	3.30	3.30	3.38	3.30	3.41	3.48	3.33
O^{2-}	25.15	25.07	25.06	24.85	24.70	24.63	24.55	24.49	24.47	24.47	24.46	24.45	24.44	24.45	24.43	24.36	24.33

single-crystal diffractometer and measuring the relative axial relations by X-ray diffraction) is as follows: X ^ **a** = 16.1°, Y ^ **b** = 16.1°, Z // **c**. Note that the optical properties have monoclinic symmetry (see discussion below).

Powder X-ray diffraction

We did not measure the powder X-ray diffraction pattern because of the compositional heterogeneity of the material (see Chemical composition). We provide a two-dimensional pattern by collapsing the three-dimensional diffraction data into two dimensions (Table 1); in this way, we can guarantee that the pattern is representative of the chemical composition and crystal structure also provided here.

Single-crystal X-ray diffraction

A single crystal was attached to a tapered glass fibre and mounted on a Bruker APEX II ULTRA three-circle diffractometer (at the University of Manitoba) equipped with a rotating-anode generator (Mo$K\alpha$), multilayer optics and an APEX II 4 K CCD detector. A total of ~10,600 intensities (the Ewald sphere) was collected to 60°2θ using 3 s per 0.2° frame with a crystal-to-detector distance of 5 cm. Empirical absorption corrections (*SADABS*, Sheldrick, 2008) were applied, Lorentz, polarization and background corrections were done, and equivalent reflections were merged, resulting in 1709 unique reflections. The unit-cell dimensions (Table 2) were obtained by least-squares refinement of the positions of 1720 reflections with $I > 10\sigma I$.

Chemical composition

Initial electron-microprobe analyses of bohseite were performed at the Inter-Institute Analytical Complex for Minerals and Synthetic Substances of the University of Warsaw with a CAMECA SX 100 electron microprobe operating in wavelength-dispersive mode (WDS) with an accelerating voltage of 15 kV, a beam current of 20 nA, peak count-time of 20 s, background time of 10 s and a beam diameter of 2 μm. Standards, analytical lines, diffracting crystals and mean detection limits (wt.%) were as follows: fluorophlogopite – F ($K\alpha$, TAP, 0.15), albite – Na ($K\alpha$, TAP, 0.01), wollastonite – Ca ($K\alpha$, PET, 0.03), orthoclase – Al ($K\alpha$, TAP, 0.01), zircon – Si ($K\alpha$, TAP, 0.02), hematite – Fe ($K\alpha$, LiF, 0.06) and rhodonite – Mn ($K\alpha$, LiF, 0.06). Iron and Mn were either below or at their limits of detection. The empirical formulae were calculated on the basis of 28 anions with BeO and H_2O iterated by stoichiometry to Be = 13–(Si + Al) and Ca + Na = Al + Be (Lussier and Hawthorne, 2011). Compositions span the range 2.84 < Be < 3.77 apfu (Table 3) and suggest that there is complete solid-solution from bavenite to close to the end-member composition of bohseite.

The crystal used for the collection of the X-ray intensity data was embedded in epoxy, ground, polished, carbon coated and analysed at the University of Manitoba with a Cameca SX-100 electron microprobe operating in WDS mode with an accelerating voltage of 15 kV, a specimen current of 15 nA and a beam diameter of 10 μm. The following standards were used: TAP: Al, andalusite; Si, diopside; LTAP: Na, albite; F, fluoro-riebeckite; LPET: Ca, diopside. The chemical composition (mean of 10 determinations) is given in Table 4. The empirical formula is as follows: $(Ca_{3.970}Na_{0.054})_{\Sigma=4.024}(Be_{3.399}Al_{0.601})_{\Sigma=4}(Si_{8.956}Al_{0.044})_{\Sigma=9}[(OH)_{3.174}F_{0.271}O_{0.555}]_{\Sigma=4}$.

Crystal-structure refinement

The structure of bohseite was refined in the space group *Cmcm* using F^2 in the *SHELXTL PLUS* (PC version) software package; initial positional parameters were those of Lussier and Hawthorne (2011). Full occupancy was assumed for all sites, and there was no subsequent indication of vacancies. The *T*(3) site is occupied by Si and Be, and the site occupancy was allowed to vary during refinement, subject to the constraint that Si + Be = 1. The constraint of electroneutrality indicates that some crystals have H present in addition to that attached to O(8), as noted by Lussier and Hawthorne (2011). This additional H,

TABLE 4. Chemical composition of crystal used to refine the structure of bohseite.

Constituent	Wt.%	Range	Stand. Dev.
SiO_2	57.41	54.69–60.02	2.20
Al_2O_3	3.51	2.91–4.17	0.56
CaO	23.75	23.53–23.91	0.14
Na_2O	0.18	0.16–0.19	0.01
F	0.55	0.39–0.75	0.12
BeO (calc)	9.07	–	–
H_2O (calc)	3.05	–	–
$O=F_2$	–0.23	–	–
Total	97.29	–	–

TABLE 5. Atom coordinates and anisotropic-displacement parameters for bohseite.

Atom	x	y	z	U^{11}	U^{22}	U^{33}	U^{23}	U^{13}	U^{12}	U_{eq}
Ca	0.08134(1)	0.26204(7)	0.15444(2)	0.01086(16)	0.01389(18)	0.00976(16)	0.00148(11)	–0.00057(10)	–0.00077(11)	0.01150(11)
T(1)	0	0.77189(17)	¼	0.0046(4)	0.0071(4)	0.0063(4)	0	0	0	0.0060(3)
T(2)	0.12393(12)	0.8292(6)	¼	0.0078(14)	0.0103(14)	0.0100(14)	0	0	–0.0001(10)	0.0094(9)
T(3)	0	0.7180(3)	0.39642(7)	0.0080(7)	0.0107(8)	0.0070(7)	–0.0005(5)	0	0	0.0086(5)
T(4)	0.09241(3)	½	0	0.0055(3)	0.0059(3)	0.0036(3)	0.0004(2)	0	0	0.00502(19)
T(5)	0.17013(3)	0	0	0.0085(3)	0.0105(3)	0.0075(3)	–0.0004(2)	0	0	0.00883(13)
T(6)	0.21379(2)	0.86856(9)	0.14481(2)	0.00714(19)	0.0091(2)	0.00740(19)	0.00071(15)	0.00081(14)	0.00036(14)	0.00789(11)
O(1)	0	0.5755(3)	0.18179(8)	0.0103(7)	0.0097(7)	0.0073(7)	–0.0007(6)	0	0	0.0091(3)
O(2)	0	0.0370(3)	0.10746(9)	0.0123(7)	0.0099(8)	0.0148(8)	0.0007(6)	0	0	0.0123(3)
O(3)	0.05770(5)	0.5939(3)	0.06791(6)	0.0140(6)	0.0170(6)	0.0131(6)	0.0013(5)	0.0046(4)	0.0045(5)	0.0147(3)
O(4)	0.13069(5)	0.2439(2)	0.03214(6)	0.0132(5)	0.0151(6)	0.0132(5)	–0.0014(5)	0.0005(4)	0.0038(4)	0.0139(2)
O(5)	0.20837(5)	0.8795(3)	0.06143(6)	0.0138(5)	0.0186(6)	0.0081(5)	0.0010(4)	–0.0003(4)	0.0028(5)	0.0135(2)
O(6)	0.23274(5)	0.5644(2)	0.16632(6)	0.0114(5)	0.0103(5)	0.0129(5)	0.0016(4)	0.0023(4)	0.0019(4)	0.0116(2)
O(7)	0.15423(5)	0.9479(2)	0.18036(6)	0.0100(5)	0.0144(6)	0.0118(5)	0.0026(4)	0.0036(4)	0.0029(4)	0.0121(2)
O(8)	0.12132(7)	0.4998(3)	¼	0.0087(7)	0.0099(7)	0.0158(8)	0	0	–0.0002(6)	0.0115(3)
O(9)	0.05769(6)	0.9610(3)	¼	0.0063(7)	0.0092(7)	0.0106(7)	0	0	–0.0007(6)	0.0087(3)
H(8)	0.1614(6)	0.437(9)	¼	0.059(14)						
H(2)	0	0.100(12)	0.0597(11)	0.07(2)						

TABLE 6. Selected interatomic distances (Å) for bohseite and selected mean values for bavenite.

Ca–O(1)		2.4993(12)	T(3)–O1		1.674(2)
Ca–O(2)		2.3733(12)	T(3)–O2		1.579(2)
Ca–O(3)		2.4115(13)	T(3)–O3	x2	1.628(2)
Ca–O(4)		2.6380(13)	<T(3)–O>		1.627
Ca–O(7)		2.3510(12)			
Ca–O(8)		2.3844(11)	T(4)–O3	x2	1.6133(12)
Ca–O(9)		2.4414(11)	T(4)–O4	x2	1.6679(12)
<Ca–O>		2.4427	<T(4)–O>		1.6406
T(1)–O(1)	x2	1.642(2)	T(5)–O4	x2	1.6374(12)
T(1)–O(9)	x2	1.633(2)	T(5)–O5	x2	1.6017(12)
<T(1)–O>		1.638	<T(5)–O>		1.6200
<bavenite>		1.636(2)	<bavenite>		1.620(4)
T(2)–O(7)	x2	1.633(2)	T(6)–O5		1.6248(13)
T(2)–O(8)		1.630(3)	T(6)–O6		1.6216(12)
T(2)–O(9)		1.669(24)	T(6)–O6		1.6283(12)
<T(2)–O>		1.641	T(6)–O7		1.5938(12)
<bavenite>		1.646(2)	<T(6)–O>		1.6171
			<bavenite>		1.618(1)

attached to the O atom at the O(2) site, was identified on a difference-Fourier map, and the H positions were refined with the soft constraint that O–H = 0.98 Å. An extinction correction was introduced in the final stages of refinement, and the structure converged to an R_1 index of 2.17%. Final atom coordinates and anisotropic-displacement parameters are given in Table 5 and selected interatomic distances are given in Table 6. Observed and calculated structure-factors and a crystallographic information file have been deposited with the Principal Editor of *Mineralogical Magazine* and are available from http://www.minersoc.org/pages/e_journals/dep_mat.html.

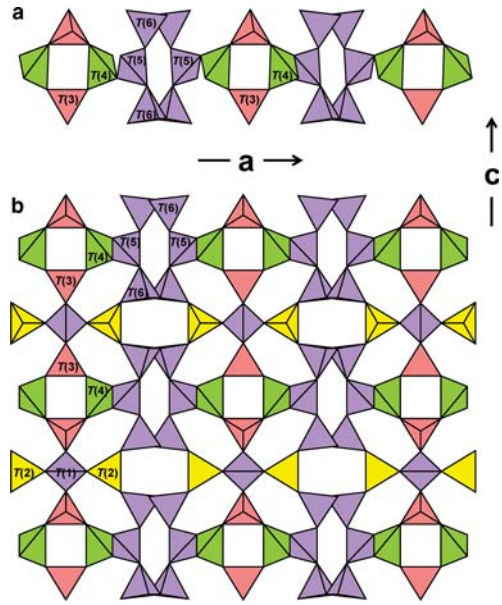

FIG. 3. The crystal structure of bohseite projected down **b**; (*a*) four-membered rings of $(Be,Si)O_4$ [*T*(3), pink] and $(Si,Al)O_4$ [*T*(4), green] tetrahedra alternating with six-membered rings of SiO_4 tetrahedra [*T*(5), *T*(6), mauve] forming a chain that extends in the **a** direction; (*b*) chain of Fig. 3a linked in the **c** direction by linear BeO_4–SiO_4–BeO_4 [*T*(2) yellow-*T*(1) mauve-*T*(2)] trimers.

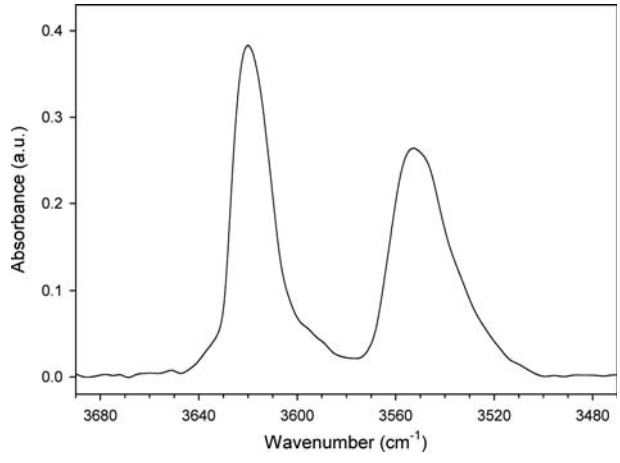

FIG. 2. The infrared spectrum of bohseite in the principal OH-stretching region.

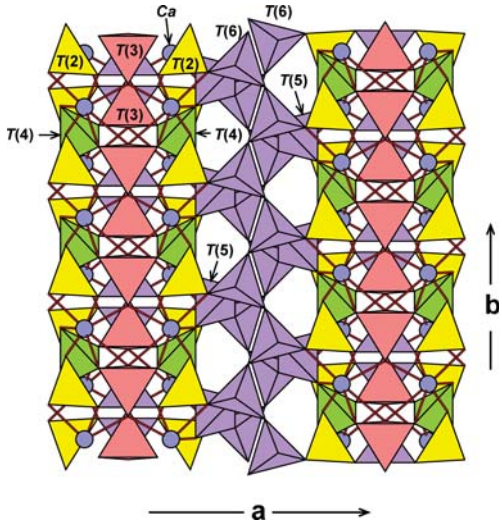

FIG. 4. The crystal structure of bohseite projected onto (001). Legend as in Fig. 3, *Ca* sites are shown by blue circles, Ca–O bonds are shown by red lines.

Fourier-transform infrared spectroscopy (FTIR)

Spectra were collected on two grains of bohseite with a Bruker Tensor 27 Fourier-transform infrared (FTIR) spectrometer equipped with an MCT detector. For each spectrum, a total of 1000 scans was collected between 4000 to 600 cm^{-1} at a resolution of 4 cm^{-1} and a beam size of 6 mm. One spectrum is shown in Fig. 2 (the other spectrum is similar). There are two relatively sharp absorptions at 3620 and 3550 cm^{-1}, in accord with the occurrence of (OH) at O(8) and O(2), respectively (Lussier and Hawthorne, 2011).

General structure description

Bohseite is isostructural with bavenite and has a framework of silicate and beryllate tetrahedra (Fig. 3). Four-membered rings of alternating $(Si,Be)O_4$ and $(Si,Al)O_4$ tetrahedra and six-membered rings of SiO_4 tetrahedra form chains extending in the **a** direction (Fig. 3*a*). Adjacent chains link through linear BeO_4–SiO_4–BeO_4 groups to form sheets that stack in the **b** direction (Fig. 4), with T(4) (= Si + Al) tetrahedra linking the sheets and [7]-coordinated interstitial Ca occupying interstices in the resulting framework.

Site populations

The <*T*–O> bond-lengths at *T*(1), *T*(2), *T*(5) and *T*(6) (Table 6) are very similar to those in bavenite (Table 2; Lussier and Hawthorne, 2011), and hence we assign *T*(1) = *T*(5) = *T*(6) = Si. Site-scattering indicates that the *T*(2) site is occupied by Be, as found by Cannillo *et al.* (1966). The <*T*(2)–O> distance of 1.641(3) Å is somewhat

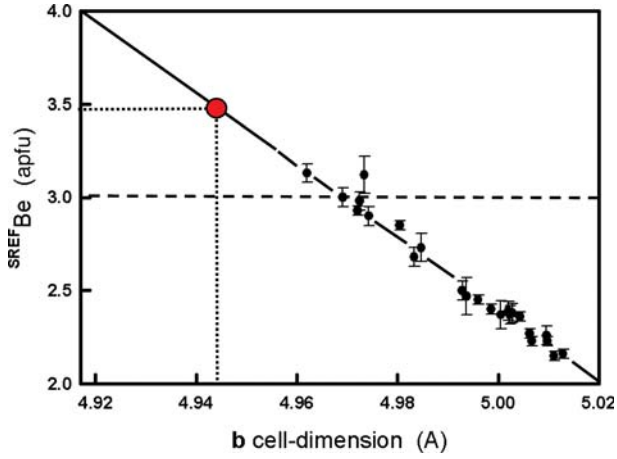

FIG. 5. Variation in ^{SREF}Be content as a function of the b cell-dimension in the bavenite-bohseite series. The data follow a linear relation (full line) to a Be content of 4 apfu at b ≈4.918 Å. The dashed horizontal line shows the line where Be = 3 apfu, and the red circle and dotted lines show the data for holotype bohseite; modified after Lussier and Hawthorne (2011).

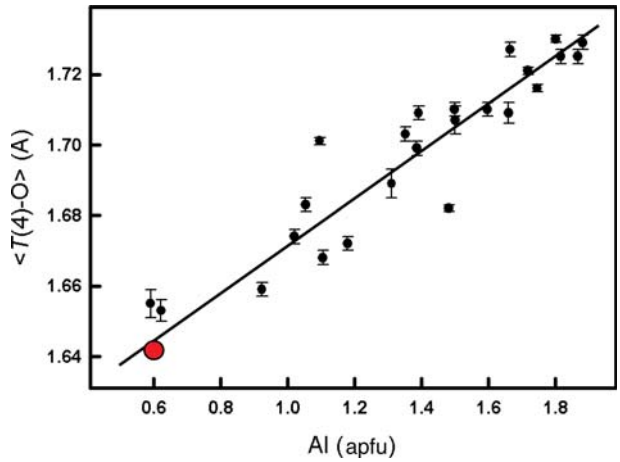

FIG. 6. Variation in <*T*(4)–O> as a function of Al in bohseite (large red circle) and the bavenite structures of Lussier and Hawthorne (2011); the bars in the latter show ± one standard deviation.

longer than the grand <Be–O> distance in minerals of 1.633 Å reported by Hawthorne and Huminicki (2002), but still lies well within the dispersion of their data. It is within the range of <*T*(2)–O> distances reported for bavenites by Lussier and Hawthorne (2011) and indicates that *T*(2) is completely occupied by Be in bohseite, as proposed by Cannillo *et al.* (1966) for bavenite. In accord with the substitution of Be for Si at the *T*(3) site in bavenite (Cannillo *et al.*, 1966; Lussier and Hawthorne, 2011), the site occupancy at the *T*(3) site was refined as (Be,Si) and gave the following site-populations (Hawthorne *et al.*, 1995): *T*(3) = 1.488(12) Be + 0.512 Si apfu. Lussier and Hawthorne (2011) noted that there is a linear relation between the Be content of the bavenite structure type and its *b* cell dimension; the data for holotype bohseite is in exact accord with this relation (Fig. 5). The <*T*(4)–O> distance of 1.641 Å is the smallest value recorded so far for the bavenite structure type, and is in accord with the $^{[4]}$Al content of bohseite derived from the chemical composition (0.601 Al apfu, Fig. 6); thus *T*(4) = 1.399 Si + 0.601 Al apfu.

TABLE 7. Comparison of the properties of bohseite and bavenite.

	Bohseite	Bavenite*
Symmetry	Orthorhombic	Orthorhombic
Sp.Gr.	*Cmcm*	*Cmcm*
a (Å)	23.204	23.209
b	4.9442	5.0129
c	19.418	19.449
Z	4	4
Colour	White	White
Streak	White	White
Cleavage	{001} Perfect, {100} Fair	{001} Perfect, {100} Fair
Hardness	5–6	5.5
Occurrence	Granitic and alkali pegmatites and veins	Granitic and alkali pegmatites and veins
End-member	$Ca_4Be_2Be_2Si_9O_{24}(OH)_4$	$Ca_4Be_2Al_2Si_9O_{26}(OH)_2$

*Cell dimensions from Lussier and Hawthorne (2011).

Compositional relations

Lussier and Hawthorne (2011) noted that the compositions Be = 3.12–3.13 apfu also have small amounts of Na replacing Ca, and suggested that the substitution Na → Ca may promote the incorporation of Be into the bavenite structure past the value of 3 apfu. Bohseite contains only minor Na replacing Ca (~0.04 Na apfu), and it is apparent that the substitution of Na for Ca in the bavenite structure type is not necessary to increase the Be content past 3 apfu. Thus there seems to be continual compositional variation from bavenite to bohseite that obeys the relation

$$^{T(4)}Si^{4+} + {}^{T(3)}Be^{2+} + {}^{O(2)}OH^{-} \rightarrow {}^{T(4)}Al^{3+} + {}^{T(3)}Si^{4+} + {}^{O(2)}O^{2-}.$$

Table 7 compares the properties of bohseite and bavenite. Specifically, bohseite has Be > 3.0 apfu and Al < 1.00 apfu; and bavenite has Be ≤ 3.0 apfu and Al ≥ 1.00 apfu.

The symmetry of bohseite

The optical properties of bohseite indicate monoclinic symmetry whereas there is absolutely no sign of monoclinic behaviour in the X-ray diffraction data. We merged the data in monoclinic symmetry three times, with a different axis designated as the unique (2-fold rotation) axis, and obtained identical R_{int} values for each merge; if there were any monoclinic aspect to the diffraction data, the unique axis would have been identified by having a lower R_{int} value. We note that the extensive crystal-structure work on bavenite has all been done in orthorhombic symmetry, whereas bavenites from different localities have been reported with orthorhombic and monoclinic optics (Petersen *et al.*, 1995).

Acknowledgements

The authors thank Peter Leverett, Gunner Raade and Daniel Atencio for their helpful comments on this paper. This work was funded by a Canada Research Chair in Crystallography and Mineralogy, an NSERC Discovery Grant, and Canada Foundation for Innovation grants to FCH, and by the National Science Centre (Poland) grant 2015/19/B/ST10/01809 to AP.

References

Armstrong, J.A., Friis, H., Lieb, A., Finch, A.A. and Weller, M.T. (2010) Combined single-crystal X-ray and neutron powder diffraction structure analysis exemplified through full structure determinations of framework and layer beryllate minerals. *American Mineralogist*, **95**, 519–526.

Bartelmehs, K.L., Bloss, F.D., Downs, R.T. and Birch, J. B. (1992) Excalibr II. *Zeitschrift für Kristallographie*, **199**, 186–196.

Berry, L.G. (1963) Composition of bavenite. *American Mineralogist*, **48**, 1166–1168.

Beus, A.A. (1966) *Geochemistry of Beryllium and Genetic Types of Beryllium Deposits*. W.H. Freeman and Co., San Francisco, California, USA.

Bondi, M., Griffin, W.L., Mattioli, V. and Mottana, A. (1983) Chiavennite, $CaMnBe_2Si_5O_{13}(OH)_2.2H_2O$, a new mineral from Chiavenna (Italy). *American Mineralogist*, **68**, 623–627.

Cannillo, E., Coda, A. and Fagani, G. (1966) The crystal structure of bavenite. *Acta Crystallographica*, **20**, 301–309.

Černý, P. (1968) Alteration of beryl in pegmatites; the process and its products. *Neues Jahrbuch für Mineralogie Abhandlungen*, **108**, 166–180.

Černý, P. (2002) Mineralogy of beryllium in granitic pegmatites. Pp. 405–444 in: *Beryllium: Mineralogy, Petrology, and Geochemistry* (E.S. Grew, editor). Reviews in Mineralogy & Geochemistry, **50**. Mineralogical Society of America and the Geochemical Society, Chantilly, Virginia, USA.

Friis, H., Makovicky, E., Weller, M.T. and Lemée-Cailleau, M.-H. (2010) Bohseite, IMA 2010-026. CNMNC Newsletter, 2010, page 800; *Mineralogical Magazine*, **74**, 797–800.

Hawthorne, F.C. and Huminicki, D.M.C. (2002) The crystal chemistry of beryllium. Pp. 333–403 in: *Beryllium: Mineralogy, Petrology, and Geochemistry* (E.S. Grew, editor). Reviews in Mineralogy & Geochemistry, **50**. Mineralogical Society of America and the Geochemical Society, Chantilly, Virginia, USA.

Hawthorne, F.C., Ungaretti, L. and Oberti, R. (1995) Site populations in minerals: terminology and presentation of results of crystal-structure refinement. *The Canadian Mineralogist*, **33**, 907–911.

Kharitonov, Yu.A., Kuz'min, E.A., Ilyukhin, V.V. and Belov, N.V. (1971) The crystal structure of bavenite. *Journal of Structural Chemistry*, **12**, 72–76.

Lussier, A.J. and Hawthorne, F.C. (2011) Short-range constraints on chemical and structural variations in bavenite. *Mineralogical Magazine*, **75**, 213–239.

Petersen, O.V., Micheelsen, H.I. and Leonardsen, E.S. (1995) Bavenite, $Ca_4Be_3Al[Si_9O_{25}(OH)_3]$, from the Ilímaussaq Alkaline Complex, South Greenland. *Neues Jahrbuch für Mineralogie Monatshefte*, **7**, 321–335.

Pieczka, A., Łodziński, M., Szełęg, E., Ilnicki, S.S., Nejbert, K., Szuszkiewicz, A., Turniak, K., Banach,

M., Michałowski, P. and Różniak, R. (2012) The Sowie Mts. pegmatites (Lower Silesia, SW Poland): a current knowledge. *Acta Mineralogia-Petrographica, Abstract series*, **7**, 105–106.

Pieczka, A., Szuszkiewicz, A., Szełęg, E., Nejbert, K., Łodziński, M., Ilnicki, S., Turniak, K., Banach, M., Hołub, W., Michałowski, P. and Różniak, R. (2013) (Fe,Mn)–(Ti,Sn)–(Nb,Ta) oxide assemblage in a little fractionated portion of a mixed (NYF + LCT) pegmatite from Piława Górna, the Sowie Mts. block, SW Poland. *Journal of Geosciences*, **58**, 91–112.

Pieczka, A., Szuszkiewicz, A., Szełęg, E., Ilnicki, Nejbert, K.,S., Turniak, K. (2014) Samarskite-group minerals and alteration products: an example from the Julianna pegmatitic system, Piława Górna, SW Poland. *The Canadian Mineralogist*, **52**, 303–319.

Sheldrick, G.M. (2008) A short history of SHELX. *Acta Crystallographica*, **A64**, 112–122.

Switzer, G. and Reichen, L.E. (1960) Re-examination of pilinite and its identification with bavenite. *American Mineralogist*, **45**, 757–762.

Szełęg, E., Szuszkiewicz, A., Pieczka, A., Nejbert, K., Turniak, K., Łodziński, M. and Ilnicki, S. (2010) Geology of the Julianna pegmatite vein system from the Piława Górna quarry (Dolnośląskie Surowce skalne S.A.), Sowie Mountains Block, SW Poland. *Mineralogia – Special Papers*, **37**, 111.

Szełęg, E., Pieczka, A., Szuszkiewicz, A., Nejbert, K., Turniak, K. and Ilnicki, S. (2013) Anomalous Be-rich bohseite from Julianna pegmatite (Piława Górna, Góry Sowie Block, Lower Silesia, Poland). *Mineralogia – Special Papers*, **41**, 85.

Szuszkiewicz, A., Szełęg, E., Pieczka, A., Ilnicki, S., Nejbert, K., Turniak, K., Banach, M., Łodziński, M., Różniak, R. and Michałowski, P. (2013) The Julianna pegmatite vein system at the Piława Górna mine, Góry Sowie Block, SW Poland – preliminary data on geology and descriptive mineralogy. *Geological Quarterly*, **57**, 467–484.

Timmermann, H., Parrish, R.R., Noble, S.R. and Kryza, R. (2000) New U–Pb monazite and zircon data from the Sudetes Mountains in SW Poland; evidence for a single-cycle Variscan Orogeny. *Journal of the Geological Society, London*, **157**, 265–268.

Van Breemen, O., Bowes, D.R., Aftalion, M. and Żelaźniewicz, A. (1988) Devonian tectonothermal activity in the Sowie Góry gneissic block, Sudetes, southwestern Poland: evidence from Rb–Sr and U–Pb isotopic studies. *Journal of the Polish Geological Society*, **58**, 3–10.